Effect of initial fabric on the undrained response of clean Chlef sand

Abdelhamid FLITTI[1*], Noureddine DELLA[1], Tim DE KOCK[2], Veerle CNUDDE[2], Ramiro Daniel VERÁSTEGUI-FLORES[3]

1. Laboratory of Material Sciences & Environment, University of Chlef (Algeria)
2. PProGRess - UGCT, Department of Geology, Ghent University (Belgium)
3. Geotechnics Division, DMOW, Government of Flanders (Belgium)
[*] Corresponding author: abdelhamid.flitti@gmail.com

Abstract

Different soil reconstitution methods lead to samples with different initial structure. This paper presents a laboratory investigation which aims to study the influence of initial fabric of specimens on the undrained behavior of clean Chlef sand subjected to triaxial compression tests. The samples tested were prepared at three level of relative densities using different deposition methods, i.e., the layered dry deposition (LDD), the tapped funnel deposition (TFD), the water deposition (WD) and the moist deposition (MD), and they were consolidated under different confining pressures. In order to evaluate the soil fabric, an analysis using X-ray µCT was conducted on three loose samples after soil reconstitution and before triaxial testing. It was found that the void ratio of the sample prepared by the moist deposition method is slightly higher than that of samples reconstituted by the two others methods (TFD and WD). The triaxial results showed that the resulting fabric affects the behavior of the sand. It was found that the effect of initial fabric is more pronounced at large strain where the specimens prepared by the moist deposition method always present the lowest resistance. These findings, especially those found at loose state, are in agreement with those obtained from µCT.

Keywords: initial fabric, undrained response, clean sand, X-ray µCT.

Nomenclature

B	Skempton coefficient ($B = \Delta u / \Delta\sigma_3$)
C_C	Coefficient of curvature ($C_C = (D_{30})^2 / (D_{60} \times D_{10})$)
C_U	Coefficient of uniformity ($C_U = D_{60} / D_{10}$)
D	Diameter of sample
D_{10}	Effective grain size diameter
D_{30}	Diameter for 30% finer by weight
D_{50}	Mean grain size diameter
D_{60}	Diameter for 60% finer by weight
Dr	Relative density
e	Void ratio
e_c	Void ratio after consolidation
e_{min}	Minimum void ratio
e_{max}	Maximum void ratio
G_S	Specific gravity of solids
H	Height of sample
Md	Dry mass of sample
V_T	Total volume of sample
p'	Effective mean stress ($q = \sigma'_1 + 2 . \sigma'_3$)
q	Deviator stress ($q = \sigma'_1 - \sigma'_3$)
q_{max}	Maximum deviator stress
σ'_c	Confining pressure
σ'_1	Major principal effective stress
σ'_3	Minor principal effective stress
LDD	Layered Dry Deposition
WD	Water deposition
TFD	Tapped Funnel Deposition
MD	Moist deposition

1. Introduction

Located close to the northern collision zone of the African tectonic plate, northern Algeria knew several earthquakes up to date. This is the case of the Chlef region that suffered two serious earthquakes in 1954 and 1980 of magnitudes 6.7 and 7.3 respectively. Liquefaction phenomena occurred in the valley of Chlef river during the last earthquake (Durville and Méneroud 1982).
Due to the geological history of the Chlef region that is classified by the Algerian seismic codes as an area of high seismicity, a detailed study of the behavior of soil from this region is a priority.
It has been reported in the literature that sample reconstitution method can significantly affect the behavior of sands (Oda 1972a, 1972b; Ladd 1974; Mulilis et al. 1977; Tatsuoka et al. 1979, 1986; Miura and Toki 1982; Zlatovic and Ishihara 1997; Jang and Frost 1998; Vaid et al. 1999; Wood and Yamamuro 1999; Høeg et al. 2000; Krim et al. 2013; Flitti et al. 2017). Many methods have been developed and tested by researchers but despite all that, their results are not always in agreement.
Many phenomena of the behavior of sand observed in the laboratory have been discussed in the past by characterizing its soil fabric created by different specimen preparation methods (Yimsiri and Soga, 2010). The term fabric refers to the arrangement of particles, particle groups, and pore spaces in a soil (Mitchell and Soga, 2005).
Based on their tests carried out on loose sandy and non-plastic silty soils, Zlatovic and Ishihara (1997) found that the effects of fabric on the undrained response are insignificant up to the peak strength, however, the fabric becomes an important factor beyond the peak. Also, they concluded that, by reaching the steady state at large shearing, the initial fabric is erased by gradual remoulding where the ultimate stress state is ruled only by the void ratio. Mulilis et al. (1977) found that reconstitution of specimens in a moist condition leads to an increase of the dynamic strength of the soil. Yamamuro and Wood (2004) found that wet deposition methods appeared to exhibit a stable response, while dry methods appeared to indicate an unstable behavior. Yamamuro et al. (2008) found that specimens formed by water sedimentation contained more stable grain contacts than those created by dry funnel deposition. By testing silty sand, Wood et al. (2008) found that the effect of the depositional method on the undrained behavior decreased with increasing density, and furthermore this effect was found to increase with silt content, particularly at lower densities. Vaid et al. (1999) presented results showing that, at identical initial void ratio and effective stress state, the moist-tamped sand is potentially liquefiable, but in the water-deposited state may even be dilative. Other researchers (Canou 1989, Benahmed et al. 2004) found that samples reconstituted by dry pluviation are more resistant than those prepared by wet tamping. By testing a natural Chlef sand, Della et al. (2009) confirmed these findings, showing that the dry funnel pluviation method gives stable samples (dilative) while the wet deposition method encourages the contractive behavior (instability of the samples).
In this research, with the aim of studying the effect of the depositional method on the undrained response of the clean Chlef sand, a series of monotonic triaxial compression tests were performed on samples prepared by several techniques of deposition.

2. Material tested

All tests in this work were carried out on clean sand taken from the Chlef river (which crosses the city of Chlef to the west of Algiers). The sand of Chlef is a medium, rounded sand with a medium diameter D_{50} = 0.596 mm. Figure 1 shows a microphotograph of clean Chlef sand and its grain size distribution curve is given in Fig. 2. The properties of the sand used in this study are illustrated in Table 1.

Fig. 1. Microphotograph of clean Chlef sand (zoom 50x)

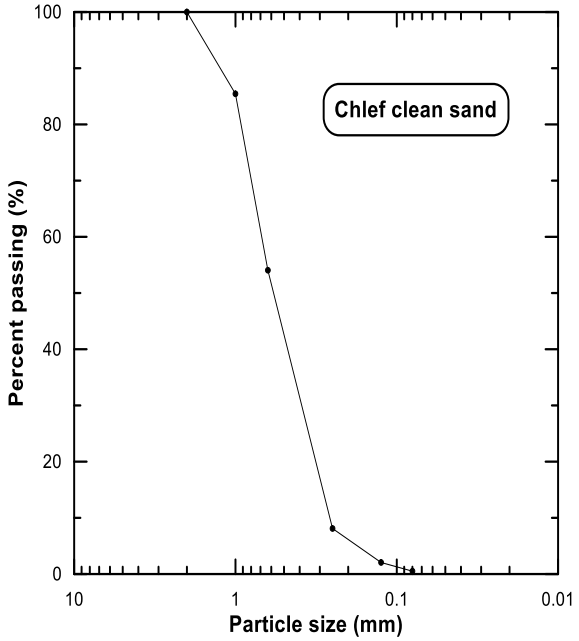

Fig. 2. Grain size distributed curve of clean Chlef sand

Table 1 Index properties of clean Chlef sand

Material	clean Chlef sand
G_S (g/cm^3)	2.652
e_{min}	0.632
e_{max}	0.795
D_{10} (mm)	0.266
D_{30} (mm)	0.431
D_{50} (mm)	0.596
D_{60} (mm)	0.700
C_U	2.634
C_C	0.999

3. Experimental program

Using a triaxial device, a series of undrained monotonic compression tests were performed on clean Chlef sand. The dimensions of samples were around 38 mm in diameter and 76 mm in height (H/D = 2). Specimens were prepared at three level of densities, dense, medium dense and loose state (Dr = 88%, 55% and 20% respectively) using different methods of preparation. Given the target density Dr, the maximum and minimum void ratio (e_{max} and e_{min}), the needed dry sand mass Md can be calculated using the two following formulas:

$$Dr = (e_{max} - e) / (e_{max} - e_{min}) \quad (1)$$

$$Md = (G_S \,.\, V_T) / (1+e) \quad (2)$$

3.1 Method of specimen preparation

To study the effect of the depositional method, four methods were chosen to produce samples with different initial fabric: the layered dry deposition, the tapped funnel deposition, the water deposition and the moist deposition.

Dry methods

Dry samples were formed by two methods. In the first method, named Layered Dry Deposition, **LDD**, the dry sand was divided into seven layers of equal height, and each layer was gently manually compacted with a tamper to achieve the dense state. Surface leveling of these layers was sufficient to achieve the medium dense state. There was no loose state sample preparation with the LDD method. In the second method, the dry sand was poured in a funnel which was placed on the bottom of the split mold, after which it was slowly raised without

any drop height (the drop height was kept almost zero as much as possible, fig. 3a). To reach higher densities, the outside of the split mold was tapped in a symmetrical pattern, and no tapping was needed to achieve the loose state. A similar technique was used by Wood et al. (2008) who named this method Tapped Funnel Deposition, **TFD.** In addition, less tapping was needed to create denser samples by increasing the speed of rising, also without using any drop height.

Water Deposition (WD) (fig. 3b)

The principle of this technique is to deposit the dry sand into water. First, the mold was half filled with water (the first quantity of water was the calculated one to reach 100% of saturation). The sand was divided in four layers. For the two first layers, the sand was deposited into water using a funnel with a plastic tube attached at the end (the nozzle tube is 4 mm in diameter). Because the surface of the second layer usually came close to the water surface, water was added before the deposition of the third layer and similar for the fourth layer. In summary, for each layer, the dry sand was poured into water through a nozzle tube from just above water surface.
To reach the dense state, each layer was gently manually compacted with a tamper, while only surface leveling was necessary to reach the medium dense state. For the loose state, the sample was not divided into layers and the sand was deposited into water in one single stage with the help of the funnel.

Moist Deposition (MD) (fig. 3c)

In this method, the dry sand was mixed with water to reach 3% of initial water content until a homogeneous sample was obtained. Then, the wet sand was deposited in seven layers of equal height (similar methods were used by Ishihara 1993; Zlatovic and Ishihara 1997; Benahmed et al. 2004; Della et al. 2009, 2014). For the dense state, each layer underwent around 125 blows using a tamper in five places (four in the periphery and one in the middle) and the blows were done by hitting the top of the tamper with a metal piece. To insure quite similar blow energy, the falling height of the metal piece and the applied force must remain constant as much as possible. For the medium dense and the loose state, compaction with the tamper was done without blows (only by using the hand force). The height of each layer must reach its desired height which is marked in the inside face of the split mold.

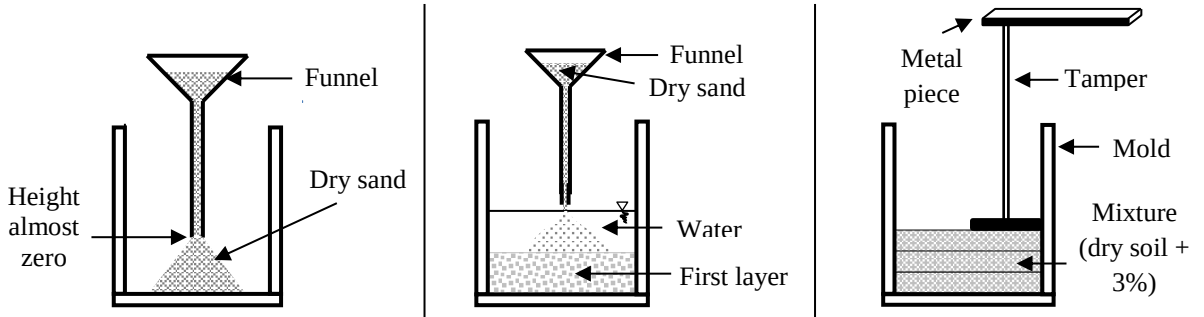

(a) Tapped Funnel Deposition method (**TFD**)

(b) Water Deposition method **(WD)**

(c) Moist Deposition method **(MD)**

Fig. 3. Sample preparation methods.

3.2 Evaluation of the initial state of the samples through X-ray tomography

To understand the fabric effect and to study the difference in initial structures of samples, three soil specimens were analyzed by means of X-ray computed microtomography (µCT). Originally, X-ray CT was developed and applied for medical applications. Then, it spread widely where it has become used in many disciplines. Mukunoki et al. (2004) counted many researchers who used the X-ray CT scanner in the geotechnical field (Peyton et al. 1992; Anderson and Hopmans 1994; Otani et al. 2002a; Anderson et al. 1992; Heijs et al. 1995; Sugawara et al. 1998; Otani et al. 2001b; Wong and Wibowo 2000) and recent state of the art is summarized by Cnudde and Boone (2013).
Desrues et al. (1996) used computed tomography to study the strain localization in triaxial tests on sand. Thomson and Wong (2008) applied X-ray CT techniques to quantify void ratio distribution within sand specimens prepared by different reconstitution methods during undrained triaxial compression and extension.
µCt was performed by taking a series of projections (radiographs) under different angle, by means of an X-ray cone beam which allows for a magnification of the sample. A filtered back-projection algorithm was used for a

virtual 3D reconstruction of the sample, which produces 2D cross-sections (slices) through the entire volume.

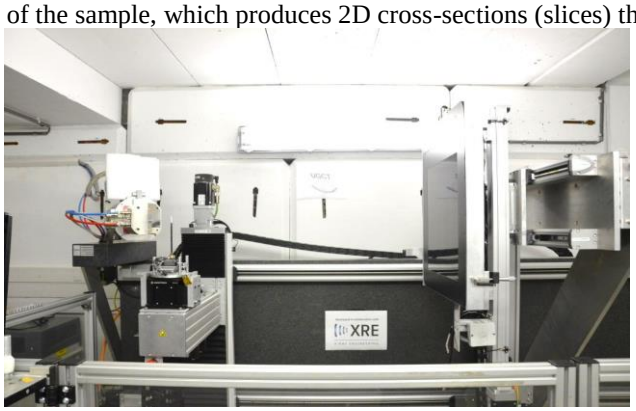

Fig. 4. Scanner (HECTOR) used in this study (UGCT)

The X-ray analysis was done using the µCT scanner HECTOR (Fig. 4) developed by UGCT (Ghent University Centre for X-ray Tomography; www.ugct.ugent.be) (Masschaele et al. 2013). The system contains three basic components; a XWT 240-SE microfocus source from X-RAY WorX, a large flat panel detector 40x40 cm² PerkinElmer 1620 CN3 CS, and a rotation stage for the sample (more details about the scanner can be found in Masschaele et al. 2013). The scans of the full volume were performed at a tube voltage of 180 kV and a power of 38 W. A 1 mm Cu filter was used to reduce beam hardening, which could also be corrected during reconstruction.

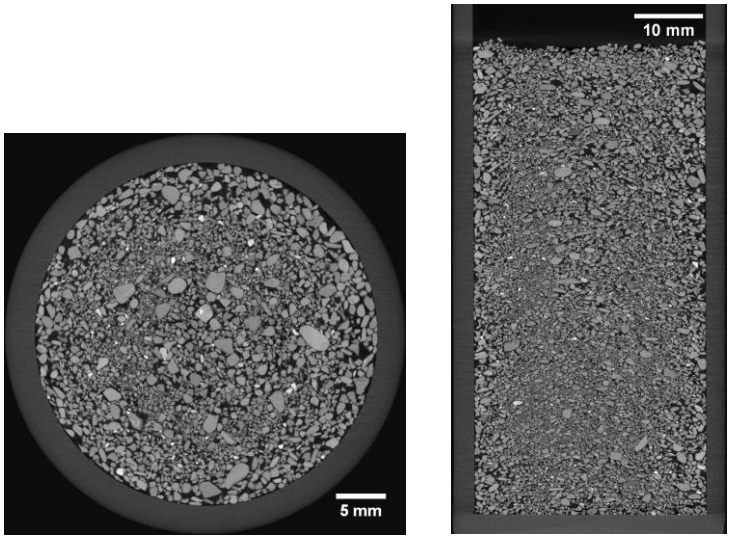

Fig. 5. Original cross section and longitudinal section of specimen prepared by the TFD method.

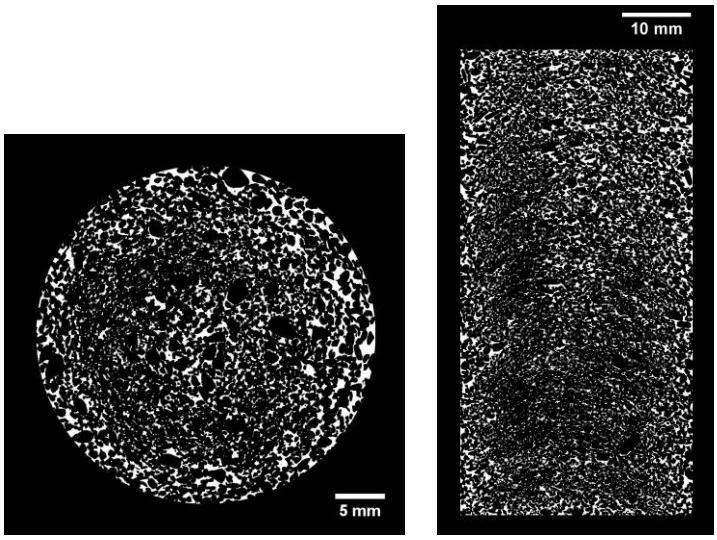

Fig. 6. Binary cross section and longitudinal section of specimen prepared by the TFD method.

In order to have accurate results on the fabric, the samples were reduced in dimension. In this case, the soil samples were reconstituted in plexiglas tubes of about 34 mm in diameter and 68mm in height, having very close dimensions to the actual soil samples tested in the triaxial cells. Before each scan, the sand was prepared in a plexiglas tube using three of the methods described in the previous section, i.e., TFD, MD and WD. The target density was lower or equal to 20% (loose state) as it was believed that differences in behavior are more pronounced at loose states. To assure good quality images, each sample was scanned in three phases from the top to the bottom (along Z axis), and to obtain the full scan of the specimen, the three parts were merged. This way, a voxel size of 40.16 µm was obtained for the full volume, at a magnification of 9.82 and detector binning of 2. The data was reconstructed using Acquila reconstruction software from XRE, and for the 3D analysis and visualization Octopus Analysis Software was used (Vlassenbroeck et al. 2007).

Diametrical cross sections and longitudinal sections were generated for all scanned samples (Fig. 5). A bilateral filter was applied to the images in order to reduce image noise. To generate binary images (Fig. 6), a volume of interest was selected (in the three directions X, Y and Z) and a dual threshold was applied to images to separate the void (white color) from the solid (black color). Using the binary images, the porosity files of the three scanned samples could be extracted.

The void ratio profiles of the three scanned specimens are shown in Fig. 7. The void ratio presented by the µCT results is smaller than the actual void ratio of the sand (e = 0.762, Dr = 20%) used in this study, which is because pore diameters (of the samples) smaller than the voxel size unit (40.16 µm) are not included in the analysis. In other words, a higher resolution scan is needed for the total of the sample to approach the real void ratio. Nevertheless, the variations of void ratio in the profiles are supposed to reflect the actual variation in the specimens. This can visually be evaluated in Figs. 5 and 6.

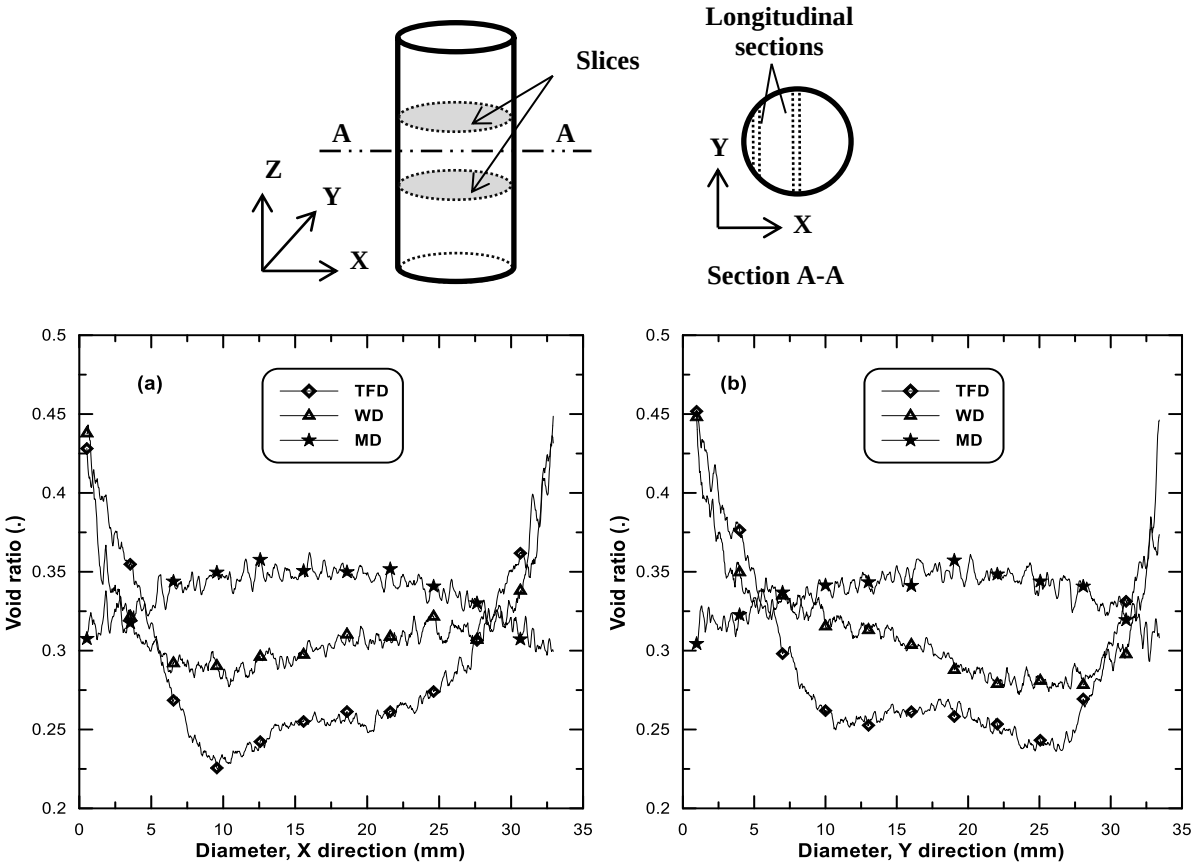

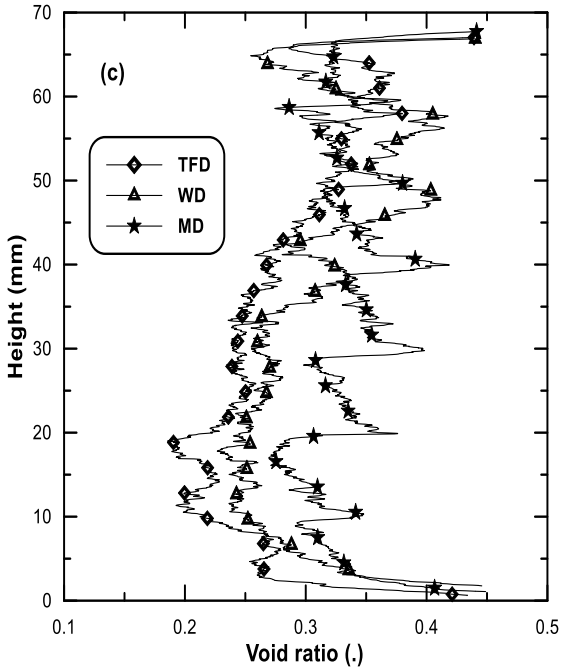

Fig. 7. Void ratio profile: (a) void ratio versus diameter (X direction); (b) void ratio versus diameter (Y direction); (c) height versus void ratio.

The distributions of the void ratio along X and Y axes are very similar (Figs. 7a and 7b) where the void ratio values presented by the MD method are greater than those exhibited by the two other methods (TFD and WD) especially in the middle where the length of the longitudinal sections is close to the sample diameter. Then, it can be seen that the density of samples formed by the TFD and WD methods is concentrated in the middle, unlike the sample created by the MD method where the density at the boundaries is a slightly higher than the density in the middle. Regarding the variation of the void ratio with the samples height, Fig. 7c shows that the density of specimens increases from top to bottom. There is a difference in the void ratio profiles; especially within the segment from 0 to 40mm in height, where the MD method shows the highest void ratio.

These results show that even if sample preparation is done carefully and targeting the same global relative density, local void ratio distribution is not uniform and it closely reflects the sample preparation procedure that was implemented. For example, the MD method, unlike the other methods, presents heterogeneous regions, areas of discontinuity in void ratio values, which coincide somewhat with the boundaries of each layer.

4. Undrained triaxial compression test

After sample preparation, a small vacuum was applied to the specimens (around -25 kPa) to reduce eventual disturbance during the removal of the split mold and triaxial cell installation. Then, the dimensions of samples were recorded (diameter and height), and after subtracting the thickness of the membrane from the diameter, the initial void ratio (before consolidation) was estimated.

When the triaxial cell was filled with water, a confining pressure up to 20 kPa was applied using a hydropneumatic system before releasing the vacuum pressure in the samples.

In the saturation stage, the dry samples were initially flushed with carbon dioxide for about 20 min. Then, de-aired water was introduced at a slow flow rate from the bottom of the sample until water drops came out from the top of the specimen. At that point, sample saturation was continued through stepwise increase of backpressure maintaining a low effective confining stress. During this process, Skempton's coefficient B was evaluated. After an increment of cell pressure was applied while drainage is not permitted, the mobilized pore water pressure in the sample is recorded. B is the ratio of the measured excess of pore water pressure and the cell pressure increase. The measured B coefficient at the end of the saturation phase for all samples was about 95%.

To consolidate the samples, the confining pressure was increased to the proposed levels. A volume change transducer was used to quatify the change in specimen volume during consolidation by measuring the volume of water evacuated from the sample. Therefore, the void ratio after consolidation can be estimated.

After that, the specimens were compressed using a strain rate of 0.1 mm/min until an axial strain of about 25% was obtained. The strain rate was kept constant for all tests. The testing program is summarized in Table 2.

Table 2 Summary of testing program

Density	Confining pressure	Preparation method	Void ratio e_c (After consolidation)
Dense state (Dr = 88%)	σ'_c = 50 kPa	LDD	0.607
		WD	0.615
		TFD	0.636
		MD	0.639
	σ'_c = 100 kPa	LDD	0.598
		WD	0.604
		TFD	0.599
		MD	0.610
	σ'_c = 200 kPa	LDD	0.593
		WD	0.595
		TFD	0.604
		MD	0.618
Medium dense state (Dr = 55%)	σ'_c = 100 kPa	LDD	0.652
		WD	0.661
		TFD	0.669
		MD	0.650
Loose state (Dr = 20%)	σ'_c = 100 kPa	WD	0.694
		TFD	0.710
		MD	0.721

5. Results and discussions

The effect of the initial fabric was studied in this work under three confining pressures at three levels of densities in order to evaluate the combined effect of the initial fabric and the two other parameters (σ'_c & Dr) on the undrained behavior of clean sand.

- **Impact of confining pressure**

To study the effect of fabric at various confining pressure (σ'_c = 50, 100 and 200 kPa), dense samples (Dr =88%), prepared by the four methods (LDD, TFD, WD, MD), were tested. Figures 8 to 10 show the undrained compression tests results of the dense samples.

The relation between the deviator stress and the axial strain is illustrated in the Figs. 8a, 9a and 10a. It can be seen that, for all methods, the deviator stress increases with increasing axial strain. At the beginning of test (between around 0 % and 1.5 % of axial strain), no significant change can be found in the deviator stress values and the effect of fabric on the undrained response of sand is negligible. After that, the difference in the deviator stress values becomes more pronounced with the development of axial strain. In general and at larger strain, for the three confining pressure, the samples prepared by the dry methods (LDD & TFD) show the highest deviator stress and the specimens formed by the moist deposition method (MD) present the lowest deviator stress. Samples reconstituted with dry methods are clearly more dilative than the other. These differences may be attributed to the different soil fabrics that result from each sample preparation method.

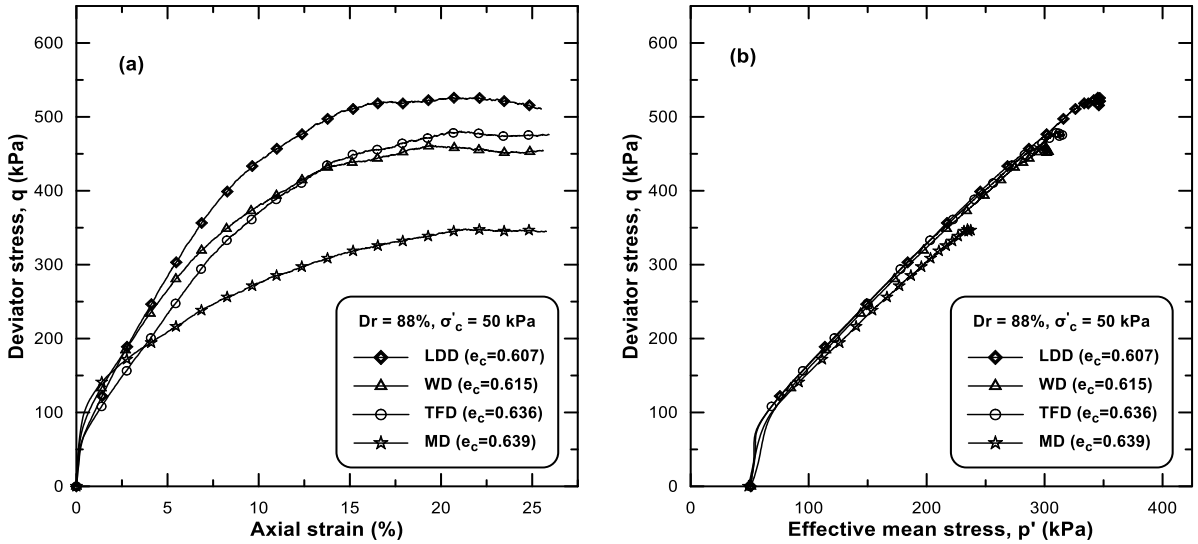

Fig. 8. Undrained triaxial tests results of dense specimens (Dr = 88%, σ'_c = 50 kPa): (a) deviator stress versus axial strain; (b) effective stress paths on Cambridge p'- q diagram.

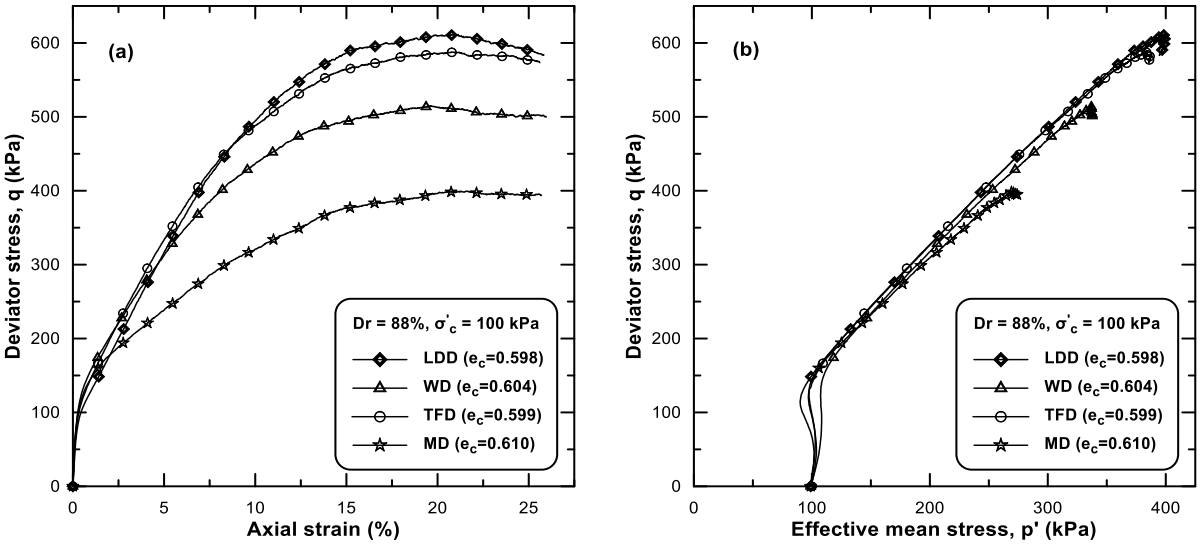

Fig. 9. Undrained triaxial tests results of dense specimens (Dr = 88%, σ'_c = 100 kPa): (a) deviator stress versus axial strain; (b) effective stress paths on Cambridge p'- q diagram.

Figures 8b, 9b and 10b show the effective stress paths on the Cambridge p'–q diagram in which $p' = (\sigma'_1 + 2\sigma'_3)/3$ and $q = \sigma'_1 - \sigma'_3$. It is clear that all samples present contractive behavior for a while in the beginning of test followed by dilative behavior which continues until the end of test. Then, it is noticed that the contractive phase becomes more significant with increasing confining pressure for all methods. From the stress-strain curves and the stress paths, it is clear that the resulting behavior of soil, defined by its initial fabric, is not further affected by an increase in confining stresses within the range from 50 to 200 kPa (Figs. 8, 9 and 10) Samples reconstituted by the dry methods keep showing the highest resistance and specimens created by the MD method exhibit the lowest one.

Figure 11 shows the variation of the deviator stress (q) corresponding to the phase transformation (transition point from contractive to dilative behavior) and the maximum deviator stress (q_{max}) with the confining pressure (σ'_c). It is clear that the difference in q values at the phase transformation is small for each confining pressure which means that the effect of fabric on the undrained behavior of sand is limited at this stage (Fig. 11a). Beyond the phase transformation at large strain, a maximum value of deviator stress is reached where the difference in q_{max} values, presented by the preparation methods, becomes significant for the three confining pressures (Fig. 11b). Although the recorded q_{max} values might be affected by shear bands developing at such large strains, they provide a qualitative means of comparing the soil response and level of dilatancy.

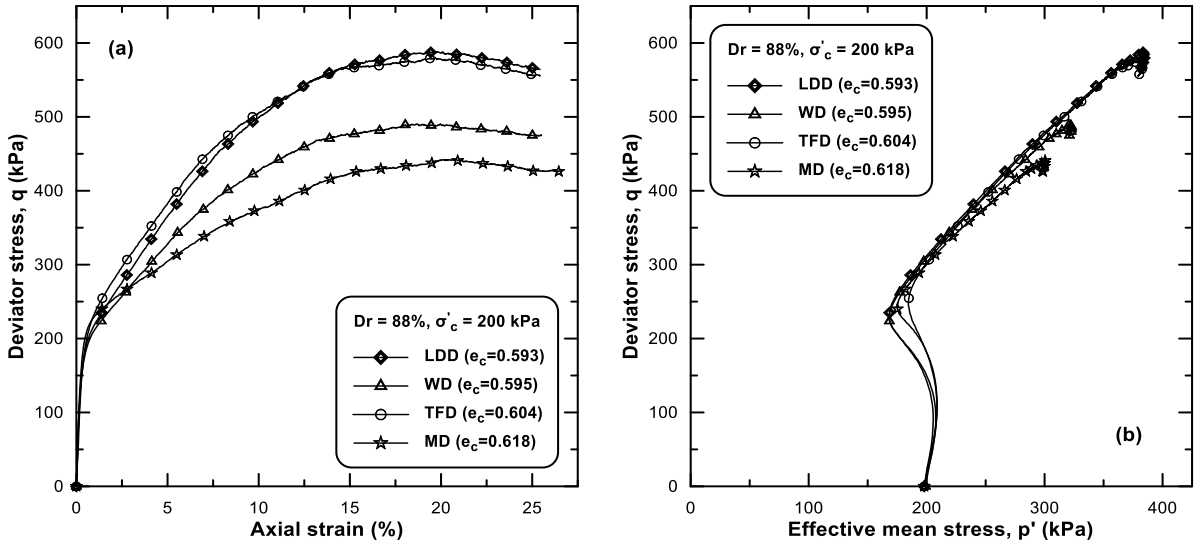

Fig. 10. Undrained triaxial tests results of dense specimens (Dr = 88%, σ'_c = 200 kPa): (a) deviator stress versus axial strain; (b) effective stress paths on Cambridge p'- q diagram.

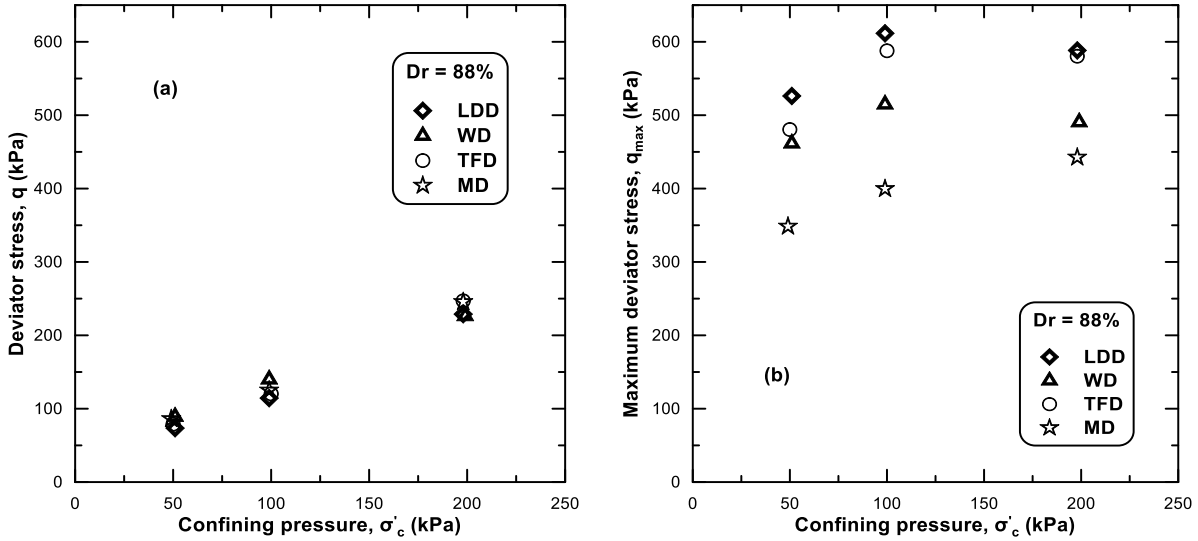

Fig. 11. Deviator stress versus confining pressure (Dr = 88%): (a) q at phase transformation vs σ'_c ; (b) q_{max} vs σ'_c.

- **Impact of the density**

To study the impact of density, specimens were tested at another two relative densities (Dr= 20%, 55%) under a common confining pressure equal to 100 kPa in order to compare them to the results obtained from the dense specimens (Fig. 9).

Figures 12a and 13a show the stress-strain curves of the medium dense and the loose state respectively. It is clear that the deviator stress for all methods increases rapidly between around 0% and 1.5% of axial strain approximately and no difference in behavior was noticed. After that, the deviator stress continues to increase with the increasing axial strain. As before, it is at large strains that these stress-strain curves seem to reflect the different soil fabric of the specimens. At large strain, the specimen prepared by the layered dry deposition (LDD) method gives the highest deviator stress (for the medium dense state). The deviator stress values of samples created by the tapped funnel deposition and the water deposition are very similar for the two densities (Dr=20% & and 55%), and the specimens formed by the moist deposition present the smallest deviator stresses.

As illustrated in the stress paths (Figs. 12b & 13b), samples initially show a contractive behavior followed by a dilative behavior until the end of test. Also, it is noticed that the dilation phase of sample prepared by the moist deposition in the loose state is very limited compared with that of specimens formed by the tapped funnel deposition and the water deposition methods.

The weak resistance of the samples reconstituted by the moist deposition method, especially at the loose state, might be explained using the µCT results, which showed that the MD method presents heterogeneous regions in

the void ratio profile with peaks and valleys oscillating around an average void ratio value that on its own is slightly higher than the void ratio achieved with other sample reconstitution methods.

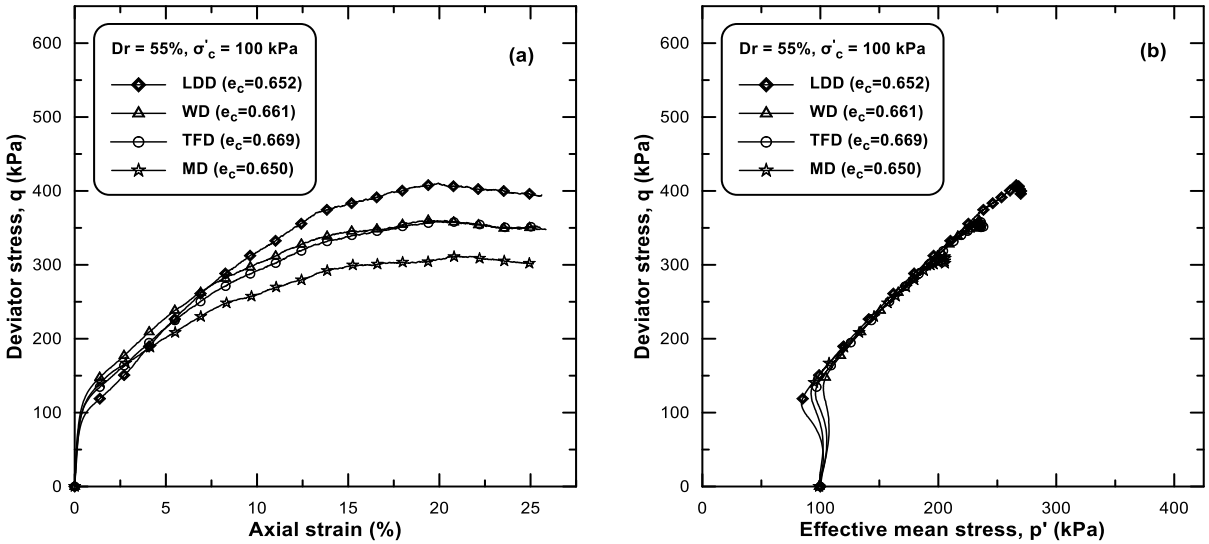

Fig. 12. Undrained triaxial tests results of medium dense specimens (Dr = 55%, σ'_c = 100 kPa): (a) deviator stress versus axial strain; (b) effective stress paths on Cambridge p'- q diagram.

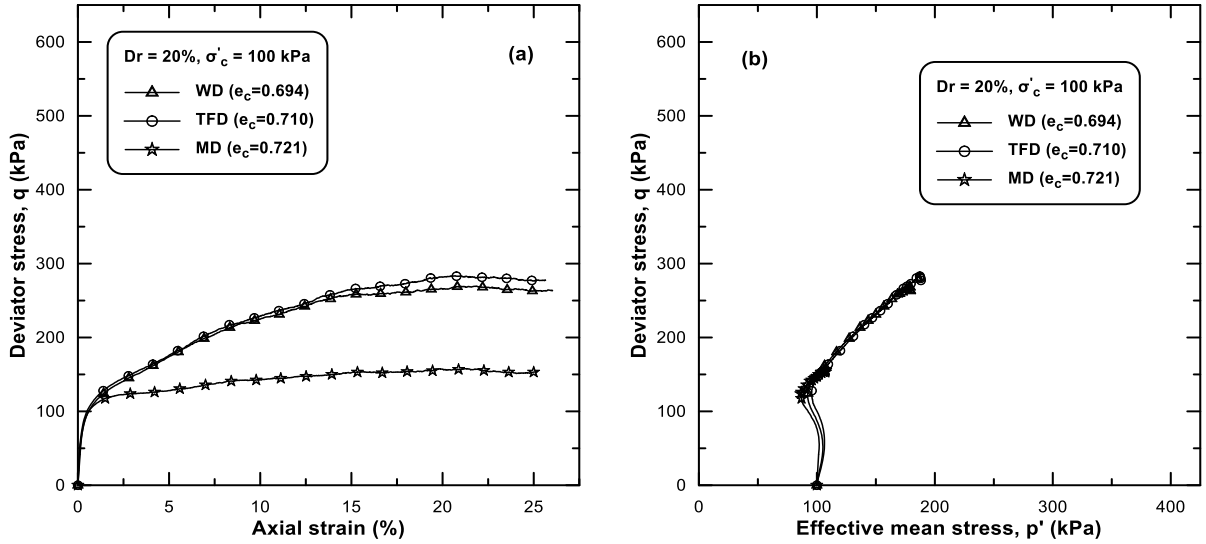

Fig. 13. Undrained triaxial tests results of loose specimens (Dr = 20%, σ'_c = 100 kPa): (a) deviator stress versus axial strain; (b) effective stress paths on Cambridge p'- q diagram.

The variation of the deviator stress (q) corresponding to the phase transformation and the maximum deviator stress (q_{max}) with the relative density is shown in Fig. 14. It can be seen in Fig. 14a that the effect of fabric on the undrained response of clean sand is insignificant before the phase transformation where the differences in the deviator stress values are small. However, the fabric effect appears and becomes very important at large strain for each relative density (Fig. 14b). Same trends were observed in the impact of confining pressure (Fig. 11).

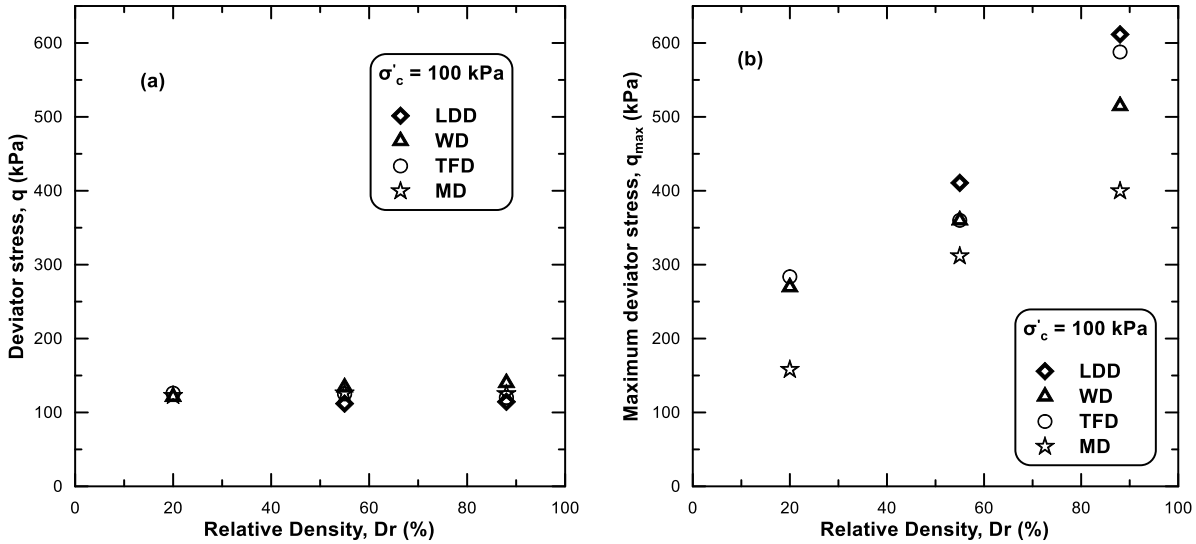

Fig. 14. Deviator stress versus relative density (σ'_c = 100 kPa): (a) q at phase transformation vs Dr ; (b) q_{max} vs Dr.

Conclusion

This paper presents a laboratory study of the effect of the initial fabric (or the depositional method) on the undrained response of clean sand collected from the Chlef river.

To reconstitute samples with different initial fabric, fours methods of preparation were chosen; the layered dry deposition (LDD), the tapped funnel deposition (TFD), the water deposition (WD) and the moist deposition (MD). In order to evaluate the initial fabric of specimens, a study with the X-ray µCT was conducted. Three loose samples prepared by different reconstitution methods (TFD, WD and MD) were scanned. It was found that the void ratio values of the sample prepared by MD method are generally greater than those of the samples created by the two other methods (TFD and WD). Additionally, it was observed that the MD method presents areas of discontinuity in the void ratio profile that correspond to the interface between sublayers.

To study the undrained response of sand samples that were created by the several methods, a series of undrained monotonic compression tests were performed using the triaxial device. The samples were tested at three level of densities (Dr = 20%, 55% and 88%) under a confining pressure of 100 kPa. For the dense state, two more values of confining pressure were evaluated (50 kPa and 200 kPa).

Tests show that the different fabrics resulting from each sample preparation method affect the behavior of clean sand. No major differences in stress-strain response among (either wet or dry) reconstituted specimens were observed at low strain levels, before phase transformation, irrespective of effective confining stress and relative density. However, the effect of fabric on the undrained behavior of sand becomes more pronounced at larger strains where the specimens reconstituted by the dry methods present the highest resistance and tendency to dilate while the samples prepared by the moist deposition method exhibit the lowest response.

The weaker response of samples reconstituted by the moist deposition method, especially at the loose state, might be explained by the highly heterogeneous void ratio profile (out of X-ray µCT scan) with peaks and valleys oscillating around an average void ratio value that on its own is slightly higher than the void ratio achieved with other sample reconstitution methods.

Acknowledgements

The first author acknowledges the support of the laboratory of geotechnics at the Catholic University of Louvain where the triaxial tests were performed during a research stage. Financial support from the Ministry of Higher Education and Scientific Research of Algeria (MESRS) is also acknowledged.

References

Anderson, S.H., Peyton, R.L., Wigger, J.W., and Ganzer, C.J. 1992. Influence of aggregate size of solute transport as measured using computed tomography. Geoderma, 53: 387–398.

Anderson, S.H., and Hopmans, J.W. 1994. Tomography of soil-water-root processes, SSSA special Publication number 36, Soil Science Society of America.

Benahmed, N., Canou, J., Dupla, J.C. 2004. Structure initiale et propriétés de liquéfaction statique d'un sable. C. R. Mecanique 332, p. 887–894.
Canou, J. 1989. Contribution à l'étude et à l'évaluation des propriétés de liquéfaction d'un sable. Thèse de Doctorat de l'Ecole Nationale Des Ponts et Chaussées, Paris.
Cnudde, V., and Boone, M.N. 2013. High-resolution X-ray computed tomography in geosciences: a review of the current technology and applications. Earth-Science Reviews, 123: 1-17.
Della, N., Arab, A., Belkhatir, M., Missoum, H. 2009. Identification of the behavior of the Chlef sand to static liquefaction. C. R. Mecanique 337, p. 282–290.
Della, N., Belkhatir, M., Arab, A., Canou, J., & Dupla, J. C. (2014). Effect of fabric method on instability behavior of granular material. Acta Mechanica, 225(7), 2043-2057.
Desrues, J., Chambon, R., Mokni, M., and Mazerolle, F. 1996. Void ratio evolution inside shear bands in triaxial sand specimens studied by computed tomography. Géotechnique, 46 (3): 529–546.
Durville, J.L., and Méneroud, J.P. 1982. Phénomènes géomorphologiques induits par le séisme d'El Asnam, Algérie, Comparaison avec le séisme de Campanie, Italie. Bull. liaison Labo P. et Ch., 120, juillet-août, p. 13-23.
Flitti, A., Della, N., and Verástegui Flores, R.D. 2017. Experimental study of the shear resistance of granular material: influence of initial state. Journal of Theoretical and Applied Mechanics, 55, 2, pp. 523-533. DOI: 10.15632/jtam-pl.55.2.523.
Heijs, W.J., Anton Lange, J., de Schoute, J.F.Th., and Bouma, J. 1995. Computed tomography as a tool for non-destructive analysis of flow patterns in macroporous clay soils. Geoderma, 64: 183–196.
Høeg, K., Dyvik, R., and Sandbækken, G. 2000. Strength of undisturbed versus reconstituted silt and silty sand specimens. Journal of Geotechnical and Geoenvironmental Engineering, 126(7): 606–617. doi:10.1061/(ASCE)1090-0241(2000)126:7(606).
Ishihara, K. 1993. Liquefaction and flow failure during earthquakes. Géotechnique, 43(3), 351-415.
Jang, D.-J., and Frost, J.D. 1998. Sand structure differences resulting from specimen preparation procedures. In Proceedings of the Specialty Conference on Geotechnical Earthquake Engineering and Soil Dynamics, Seattle, Wash., American Society of Civil Engineers, Vol. 1, pp. 234–245.
Krim, A., Zitouni, Z., Arab, A., and Belkhatir, M. 2013. Identification of the behavior of sandy soil to static liquefaction and microtomography. Arabian Journal of Geosciences, 6(7), pp. 2211–2224.
Ladd, R.S. 1974. Specimen preparation and liquefaction of sands. Journal of Geotechnical Engineering, 100(GT10): 1180–1184.
Masschaele, B., Dierick, M., Van Loo, D., Boone, M.N., Brabant, L., Pauwels, E., Cnudde, V., Van Hoorebeke, L. 2013. HECTOR: A 240kV micro-CT setup optimized for research. Journal of Physics: Conference Series 463:012012. doi:10.1088/1742-6596/463/1/012012.
Mitchell, J. K., & Soga K. 2005. Fundamentals of Soil Behavior (3rd ed.). Hoboken, New Jersey: John Wiley & Sons.
Miura, S., and Toki, S. 1982. A sample preparation method and its effect on static and cyclic deformation-strength properties of sand. Soils and Foundations, 22(1): 61–77.
Mukunoki, T., Otani, J., Obara, Y., Kaneko, K. 2004. Artifacts of X-ray CT data in the analysis of geomaterial properties. In: Otani J. & Obara Y. (Eds.), X-ray CT for Geomaterials; Soils, Concrete, Rocks. Swets & Zeitlinger, Lisse, pp. 95-101.
Mulilis, J.P., Seed, H.B., Chan, C.K., Mitchell, J.K., and Arulanandan, K. 1977. Effects of sample preparation on sand liquefaction. Journal of Geotechnical Engineering, 103(GT2): 91–108.
Oda, M. 1972a. Initial fabrics and their relations to mechanical properties of granular material. Soils and Foundations, 12(1): 17–36.
Oda, M. 1972b. The mechanism of fabric changes during compressional deformation of sand. Soils and Foundations, 12(2): 1–18.
Otani, J., Kikuchi, Y., Mukunoki, T., and Yamagata, N. 2001. Evaluation of hydraulic property of light weight soil with air foams, Proc. of the International Workshop on lightweight Geo-Materials, pp. 159–164.
Otani, J., Mukunoki, T., and Kikuchi, Y. 2002. Visualization for engineering property of in-situ light weight soils with air foams. Soils & Foundations the Japanese Geotechnical Society, 42 (3): 93–105.
Peyton, R.L., Haeffner, B.A., Anderson, S.H., and Ganzer, C.J. 1992. Applying X-ray CT to measure micropore diameters in undisturbed soil cores. Geoderma, 53: 329–340.
Sugawara, K., Kojima, R., Obara, Y., Sato, A., and Shimada, H. 1998. Crack opening analysis by means of the X-rays CT. Journal of the Mining and Material Processing Institute of Japan, 114 (12): 881–887 (in Japanese).
Tatsuoka, F., Iwasaki, T., Yoshida, S., Fukushima, S., and Sudo, H. 1979. Shear modulus and damping by drained tests on clean sand specimens reconstituted by various methods. Soils and Foundations, 19(1): 39–54.

Tatsuoka, F., Ochi, K., Fujii, S., and Okamoto, M. 1986. Cyclic undrained triaxial and torsional shear strength of sands for different sample preparation methods. Soils and Foundations, 26(3): 23–41.

Thomson, P.R., and Wong, R.C.K. 2008. Specimen nonuniformities in water-pluviated and moist-tamped sands under undrained triaxial compression and extension. Can. Geotech. J., 45: 939–956.

Vaid, Y.P., Sivathayalan, S., and Stedman, D. 1999. Influence of specimen-reconstituting method on the undrained response of sand. Geotechnical Testing Journal, 22(3): 187–195.

Vlassenbroeck, J., Dierick, M., Masschaele, B., Cnudde, V., Van Hoorebeke, L., and Jacobs, P. 2007. Software tools for quantification of X-ray microtomography at the UGCT. Nuclear Instruments and Methods in Physics Research Section A: Accelerators, Spectrometers, Detectors and Associated Equipment, 580: 442–445.

Wong, R.C.K., and Wibowo, R. 2000. Tomographic Evaluation of Air and Water Flow Patterns in Soil Column. Geotechnical Testing Journal, GTJODJ, Vol. 23, No. 4: 413–422.

Wood, F.M., and Yamamuro, J.A. 1999. The effect of depositional method on the liquefaction behavior of silty sand. In Proceedings of the 13th ASCE Engineering Mechanics Conference, The Johns Hopkins University, Baltimore, Md.

Wood, F.M., Yamamuro, J.A., and Lade, P.V. 2008. Effect of depositional method on the undrained response of silty sand. Canadian Geotechnical Journal, 45: 1525–1537.

Yamamuro, J.A., and Wood, F.M. 2004. Effect of depositional method on the undrained behavior and microstructure of sand with silt. Soil Dynamics and Earthquake Engineering, 24: 751–760.

Yamamuro, J.A., Wood, F.M., and Lade, P.V. 2008. Effect of depositional method on the microstructure of silty sand. Canadian Geotechnical Journal, 45: 1538-1555.

Yimsiri, S., & Soga, K. (2010). DEM analysis of soil fabric effects on behaviour of sand. Géotechnique, 60(6), 483–495.

Zlatovic, S., and Ishihara, K. 1997. Normalized behavior of very loose non-plastic soils: effects of fabric. Soils and Foundations, 37(4): 47–56.